Geological Survey
of Canada

CURRENT RESEARCH
2002-F4

In situ SHRIMP U-Pb geochronology of Barrovian facies-series metasedimentary rocks in the Happy lake and Josephine River supracrustal belts: implications for the Paleoproterozoic architecture of the northern Hearne domain, Nunavut

Robert G. Berman, William J. Davis, James J. Ryan, Subhas Tella, and Norah Brown

2002

Natural Resources Canada | Ressources naturelles Canada

Canada

ISSN No. 1701-4387

Available in Canada from the
Geological Survey of Canada Bookstore website at:
http://www.nrcan.gc.ca/gsc/bookstore (Toll-free: 1-888-252-4301)

A copy of this publication is also available for reference by depository libraries across Canada through access to the Depository Services Program's website at http://dsp-psd.pwgsc.gc.ca

Price subject to change without notice

Authors' addresses

R.G. Berman ***(rberman@nrcan.gc.ca)***
W.J. Davis ***(bidavis@nrcan.gc.ca)***
S. Tella ***(stella@nrcan.gc.ca)***
N. Brown ***(nbrown@ncc.ccn.ca)***
Continental Geoscience Division
Geological Survey of Canada
601 Booth Street
Ottawa, Ontario K1A 0E8

J.J. Ryan ***(jryan@nrcan.gc.ca)***
Continental Geoscience Division
Geological Survey of Canada
605 Robson Street, Suite 101
Vancouver, British Columbia
V6B 5J3

Publication approved by Continental Geoscience Division

In situ SHRIMP U-Pb geochronology of Barrovian facies-series metasedimentary rocks in the Happy lake and Josephine River supracrustal belts: implications for the Paleoproterozoic architecture of the northern Hearne domain, Nunavut[1]

Robert G. Berman, William J. Davis, James J. Ryan, Subhas Tella, and Norah Brown

Berman, R.G., Davis, W.J., Ryan, J.J., Tella, S., and Brown, N., 2002: In situ SHRIMP U-Pb geochronology of Barrovian facies-series metasedimentary rocks in the Happy lake and Josephine River supracrustal belts: implications for the Paleoproterozoic architecture of the northern Hearne domain, Nunavut; Radiogenic Age and Isotopic Studies: Report 15; Geological Survey of Canada, Current Research 2002-F4, 14 p.

Abstract: Sensitive high-resolution ion microprobe (SHRIMP) U-Pb dates on in situ monazite grains are interpreted to yield an age of 1886 ± 6 Ma for the approximately 6 kbar metamorphism and associated S_2 shortening within kyanite-bearing metapelitic rocks of the Josephine River supracrustal belt. These data demonstrate that mid-crustal shortening accompanied ca. 1.9 Ga, greater than 10 kbar metamorphism previously documented in the adjacent northwestern Hearne domain.

In situ SHRIMP U-Pb monazite ages for kyanite-bearing metasedimentary rocks near Happy lake, metamorphosed at approximately 6 kbar, form a single 1835 ± 11 Ma population. An apparent correlation between monazite ages and textural locations, however, is interpreted to yield 1850 ± 18 Ma for the age of Barrovian metamorphism and associated S_1 or S_2 fabric (textural ambiguity remains), and 1826 ± 15 Ma for the age of S_3 staurolite. It is suggested here that the greater than 1850 Ma, S_1 fabric is associated with a regionally important shear zone that carried the central Hearne domain northward over the northwestern Hearne domain.

Résumé : Les mesures localisées à la microsonde ionique à haute résolution et à haut niveau de sensibilité (SHRIMP) sur des cristaux de monazite contenus dans des métapélites à kyanite de la ceinture de roches supracrustales de Josephine River permettent d'attribuer, à l'aide de la méthode U-Pb, un âge de 1 886 ± 6 Ma au métamorphisme qui s'est déroulé à environ 6 kbar et à la déformation par compression associée qui a produit S_2. Ces données démontrent qu'un raccourcissement en milieu médiocrustal a accompagné, il y a environ 1,9 Ga, le métamorphisme ayant touché tout à côté la partie nord-ouest du domaine de Hearne, dont les signes précédemment rapportés révèlent qu'il s'est détroulé à une pression de plus de 10 kbar.

À partir de roches métasédimentaires à kyanite situées près du lac Happy pour lesquelles une pression de métamorphisme d'environ 6 kbar peut être établie, on a effectué des datations par la méthode U-Pb sur des cristaux de monazite par des mesures localisées à la microsonde ionique SHRIMP. Les âges déterminés par ces mesures définissent une seule population à 1 835 ± 11 Ma. Cependant, l'interprétation d'une corrélation apparente entre les âges des monazites et les sites structuraux permet d'attribuer un âge de 1 850 ± 18 Ma au métamorphisme de type barrovien et à la fabrique S_1 ou S_2 (une ambiguïté structurale persiste) associée, ainsi qu'un âge de 1 826 ± 15 Ma à la staurotide associée à S_3. Il est proposé que la fabrique S_1 remontant à 1 850 Ma ou plus soit associée à une zone de cisaillement importante à l'échelle régionale qui témoigne du transport de la partie centrale du domaine de Hearne vers le nord, sur la partie nord-ouest du domaine de Hearne.

[1] Contribution to the Western Churchill NATMAP Project

INTRODUCTION

The western Churchill Province (Fig. 1) represents a large Archean craton that formed the upper plate to both the ca. 1.97–1.91 Ga Thelon–Taltson Orogen (Hoffman, 1990) and the 1.83–1.78 Ga terminal stage of the Trans-Hudson Orogen (Ansdell et al., 1995). It has been divided into the Rae and Hearne domains by the controversial Snowbird tectonic zone (Hoffman, 1990; Ross et al., 1995; Hanmer, 1997; Sanborn-Barrie et al., 2001).

Recent work associated with the Western Churchill NATMAP Project has revealed a 'northwestern Hearne domain' (Fig. 2; Davis et al., 2000; Hanmer and Relf, 2000) that was reworked during a relatively low pressure tectonometamorphic event at 2.56–2.50 Ga, as well as a high-pressure event at 1.9 Ga (Berman et al., 2000). Within this domain, supracrustal rocks experienced approximately 6 kbar metamorphism and deformation at ca. 2.56–2.50 Ga, and approximately 10 kbar, static metamorphism at 1.9 Ga (Berman et al., 2000; Stern and Berman, 2000). In the Chesterfield Inlet area (Fig. 2), deformation appears to have generally accompanied approximately 10 kbar and approximately 13–14 kbar granulite-facies metamorphism, respectively, during these two events (Ryan et al., 2000; Mills, 2001; Sanborn-Barrie et al., 2001). Although detailed tectonic models have yet to be developed, the 2.56–2.50 Ga event is generally thought to be related to compressional reworking of the Rae–Hearne boundary (Hanmer and Relf, 2000; Davis et al., 2000; Berman et al., 2000). Interpretation of the ca. 1.9 Ga event, however, has been controversial, with the central issue being whether it was a strictly thermal event (e.g. Hanmer and Relf, 2000; Aspler et al., 2001) or an event with associated crustal thickening (Berman et al., 2000).

In order to further constrain this problem and formulate adequate tectonic models, geochronological and metamorphic data are required to establish the timing and style of metamorphism and deformation in regions adjacent to the northwestern Hearne domain. This paper presents the results of two such studies conducted on supracrustal rocks of the Josephine River belt, approximately 100 km east of the presently defined northwestern Hearne domain (Fig. 2), and near Happy lake (unofficial name) on the north flank of the Kaminak volcanic belt of the central Hearne domain (Fig. 2). These results are used to speculate about the crustal architecture of the southeastern boundary of the northwestern Hearne domain (Fig. 2).

JOSEPHINE RIVER SUPRACRUSTAL BELT

Geology

The geology of the region around the Josephine River supracrustal belt is known from previous 1:250 000 scale mapping (Tella and Annesley, 1987; Tella et al., 1992; Tella, 1993).

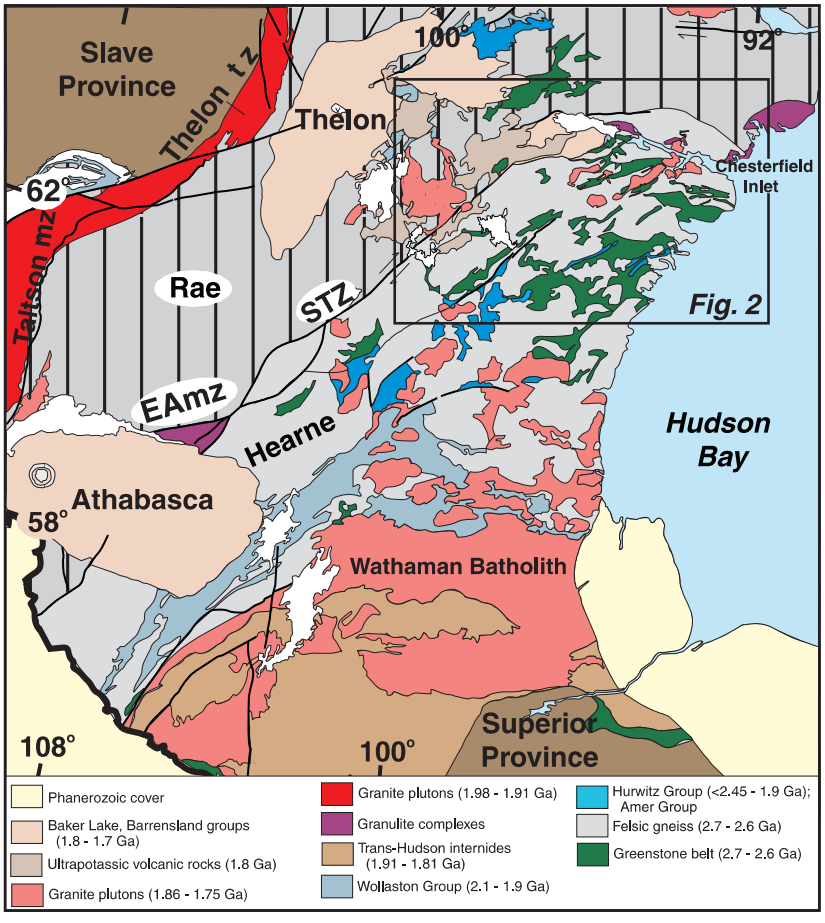

Figure 1.

*Regional geology of part of the western Churchill Province, showing the Rae and Hearne domains (*modified after *Wheeler et al., 1996). EAmz, East Athabasca mylonite zone; STZ, Snowbird tectonic zone; tz, tectonic zone; mz, magmatic zone.*

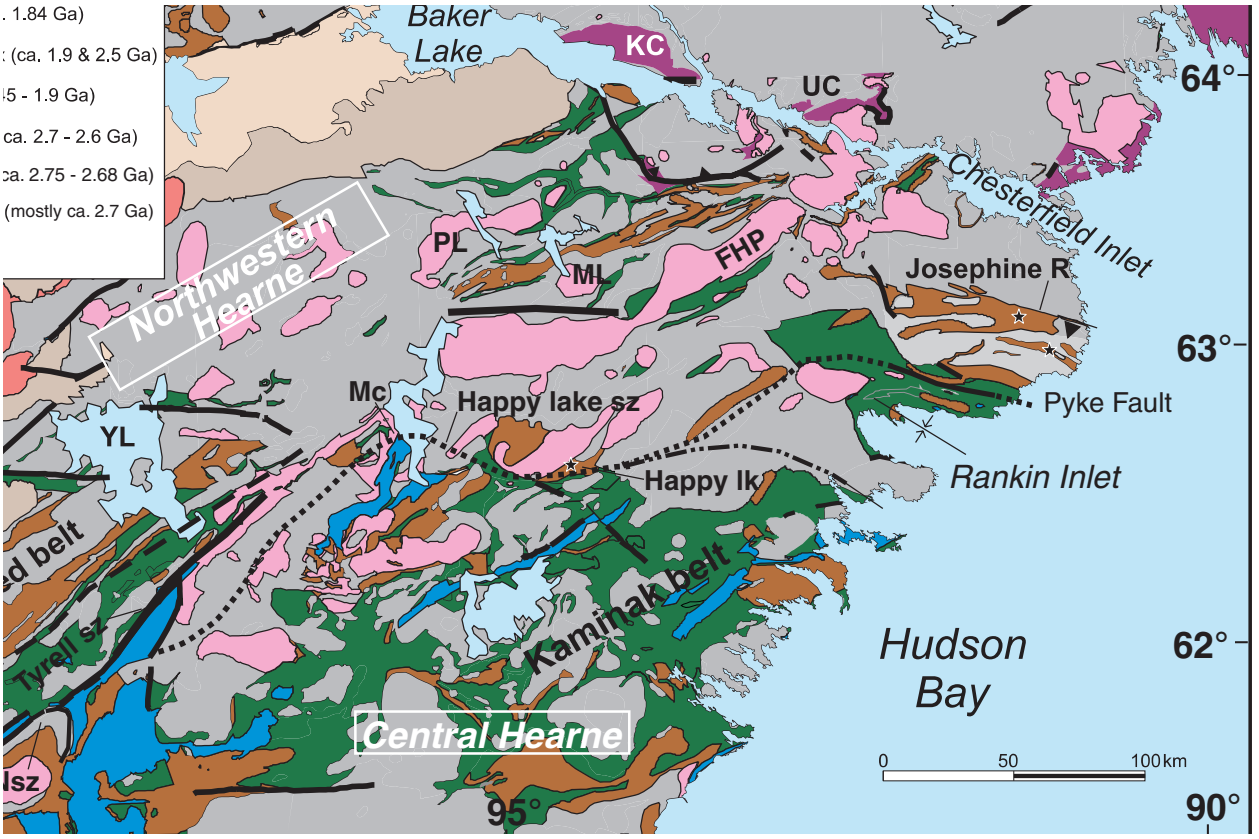

Figure 2. *Regional geology of the western Churchill Province (*modified after *Paul et al., 2002) showing the location of samples studied in the Josephine River and Happy lake supracrustal rocks. Dotted and dashed-dotted lines are possible extrapolations of the Happy lake shear zone. Asterisks indicate Happy lake and Josephine River sample localities (z7235 is south of z7234). AL, Angikuni Lake; FHP, Farther Hope Point pluton (limits eastern extent of northwestern Hearne domain); KC, Kramanituar complex; Mc, MacKenzie Lake locality (discussed in text); Nsz, Nowyak Lake shear zone; UC, Uvauk complex; YL, Yathkyed Lake.*

The area is underlain predominantly by polydeformed, granitic-tonalitic orthogneiss, together with migmatite, biotite schist, and weakly deformed, ca. 2.61 Ga, K-feldspar megacrystic granite. A series of west-northwest-trending and moderately to steeply south-dipping paragneiss belts (referred to here collectively as the Josephine River supracrustal belt) structurally overlie the orthogneiss, and have a composite width of approximately 15 km. The eastern segment of the northern paragneiss-orthogneiss contact was mapped as a north-northeast-verging thrust (Tella et al., 1992), based on the occurrence of kyanite south of the contact, together with a southwest-trending, predominantly downdip stretching lineation that characterizes rocks north of the Pyke fault (Fig. 2; see below). The paragneissic units are commonly well-banded, fine- to medium-grained, iron-rich pelitic rocks containing quartz-rich, quartzofeldspathic, and garnet- biotite-kyanite–rich layers. The supracrustal belt is intruded by weakly to well-foliated, two-mica leucogranite that contains garnet and muscovite xenocrysts as well as abundant layered gneiss and paragneiss inclusions.

The Josephine River supracrustal belt forms part of the northern limb of a shallowly (15–25°) southeast-plunging, regional F_2 syncline defined in the Rankin Inlet area (Fig. 2; Tella et al., 1986, 1992; Tella, 1994). The main foliation observed in paragneiss outcrops most commonly represents a composite S_1-S_2 fabric that is generally concordant with the layering in the underlying orthogneiss. This foliation trends west-northwest and dips steeply (70–80°) to the south, with local reversals to the north. Previous mapping in the southeastern limit of the supracrustal belt (Tella, 1995) indicates the presence of two penetrative planar fabrics. The S_1 fabric trends 270–300° and locally contains a northeast-plunging extension lineation (e.g. amphibole oriented 044°/30° within interbedded metavolcanic rocks). This extension lineation is more prominent to the south of the Josephine River belt, where its plunge is commonly toward the southwest. The S_2 fabric is axial planar to mesoscopic isoclinal folds that are locally developed on the northern limb of the regional F_2 syncline. At several localities, S_2 has a consistent clockwise

obliquity with respect to S_1, generally between 10 and 30°, and rarely up to 60°. Near the northeast flank of the supracrustal belt, east-southeast-trending, steeply dipping, discontinuous high-strain zones within the supracrustal rocks are characterized by shallowly plunging (5–15°) extension lineations, which record later displacements that are dominantly strike slip.

Metamorphism

The Josephine River supracrustal belt is characterized by Barrovian facies-series metamorphic assemblages of lower- to middle-amphibolite grade. Several thin sections of two samples from an archived regional collection (Tella and Annesley, 1987) were studied in detail. Sample z7235 (field no. 86TX-082) is a coarse-grained, kyanite-garnet-staurolite-biotite-muscovite schist interlayered with biotite paragneiss. A stretching lineation (quartz rodding), oriented at approximately 270°/30°, is associated with the main 100°/70°S foliation. Sample z7234 (field no. 86TXD-047) is a coarse-grained, kyanite-garnet-staurolite-biotite-muscovite schist with large blades of kyanite parallel to the main S_2 fabric (125°/60–80°S). The later high-strain zones were not noted at either locality.

Two planar fabrics are evident in thin sections of both samples. The S_1 fabric is a biotite-defined foliation that has been transposed into the strong, differentiated S_2 foliation predominantly observed in outcrop.The S_2 foliation is axial planar to small, near-isoclinal folds of the S_1 foliation in sample z7234 (Fig. 3a), a relationship that mimics the F_2-S_2 relationship observed at outcrop scale. In addition, sample z7235 shows a low-amplitude crenulation of the S_2 fabric that appears to be associated with retrograde chlorite growth. In both samples, garnet, kyanite, and staurolite porphyroblasts are predominantly enveloped by S_2, and contain straight to curved S_1 inclusion trails at a high angle to S_2. These relations indicate post-S_1, early S_2 porphyroblast growth. There is a significant range, however, in the intensity of alignment of S_1 inclusions in garnet porphyroblasts that may reflect growth of some garnet porphyroblasts during S_1 fabric development. Some kyanite blades within the S_2 fabric contain S_2-aligned quartz inclusions, as well as small garnet porphyroblasts with S_1 inclusion trails at a high angle to S_2 (Fig. 3b), indicating that kyanite continued to grow throughout S_2 fabric development.

Chemical profiles of garnet porphyroblasts from both samples are shown in Figures 4a and 4b. There is very little variation in CaO (mole fraction of grossular in garnet [X_{Grs}] <0.01), except for a small core to rim decrease (X_{Grs} = 0.066–0.049) in porphyroblast A of z7234 (Fig. 4b). The Fe/(Fe+Mg) ratio and X_{Mn} are also fairly uniform, with some garnet rims having increased Fe/(Fe+Mg) and X_{Mn} that may be related to retrograde re-equilibration. No significant chemical variations with textural location are displayed by biotite (Fe/[Fe+Mg] = 0.45–0.48) or plagioclase (X_{An} = 0.25–0.27), with the exception of more calcic (X_{An} = 0.35) plagioclase inclusions found in garnet porphyroblast B of z7234, which has a flat CaO profile (Fig. 4b). Although more

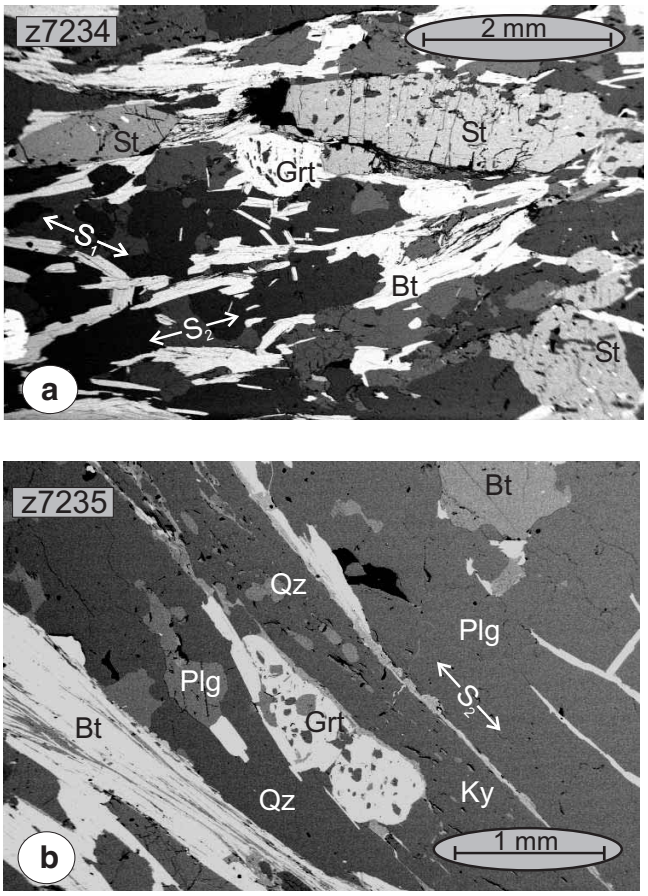

Figure 3. *Scanning electron microscope images of porphyroblast-fabric relationships in Josephine River samples:* ***a)*** *z7234, in which S_2 is axial planar to folded S_1 fabric that is also included in porphyroblasts of garnet and staurolite;* ***b)*** *z7235, in which S_2-aligned kyanite occurs with S_2-aligned quartz and garnet inclusions. Bt, biotite; Grt, garnet; Ky, kyanite; Plg, plagioclase; Qz, quartz; St, staurolite.*

detailed work is needed to establish pressure-temperature (P-T) paths, the above compositional trends in garnet and plagioclase suggest single-stage, prograde garnet growth with increasing pressure (P-T gradient somewhat steeper than barometer isopleths shown in Fig. 4c).

Pressure-temperature estimates were calculated using the TWQ software program (Berman, 1991), with the version 1.02 thermodynamic database (Berman, 1992). Mineral compositions (Table 1) were obtained using procedures described by Berman and Bostock (1997). Near-peak P-T results (Fig. 4c), calculated with garnet rims and adjacent plagioclase and biotite, are 575°C and 5.5 kbar for sample z7235, and 600°C and 6.3 kbar for sample z7234. Prograde conditions could not be calculated because garnet porphyroblasts do not contain 'armoured' biotite inclusions that were isolated from retrograde Fe-Mg re-equilibration.

Table 1. Thermobarometric data and mineral compositions, samples z7234 and z7235.

	z7234 (6.3 kbar, 600°C)				z7235 (5.5 kbar, 575°C)			
P-T[1]	Grt	Bt	Ms	Plg	Grt	Bt	Ms	Plg
Na_2O	-	0.10	0	8.40	-	0.30	1.1	9.20
K_2O	-	8.50	8.6	0.10	-	8.80	8.1	0.10
FeO	33.90	17.30	0.8	-	35.00	17.60	0.8	-
MgO	3.60	10.80	0.6	-	3.50	10.70	0.4	-
CaO	2.20	-	-	5.30	1.60	-	-	4.30
MnO	1.30	0.10	-	-	2.30	0.10	0.1	-
SiO_2	36.90	34.00	42.7	61.50	37.10	35.70	45.7	63.20
TiO_2	-	1.70	0.6	-	-	1.90	0.4	-
Al_2O_3	21.10	18.20	34.9	24.00	21.20	18.50	36.2	23.00
Total	99.00	90.70	88.20	99.30	100.70	93.60	92.80	99.80

[1]calculated with TWQ (v. 1.02) software from average intersection of equilbria (1), (2), and (3):
(1) almandine + phlogopite = pyrope + annite
(2) grossular + 2 kyanite + quartz = 3 anorthite
(3) annite + 3 anorthite = grossular + almandine + muscovite
Abbreviations: Bt, biotite; Grt, garnet; Ms, muscovite; Plg, plagioclase

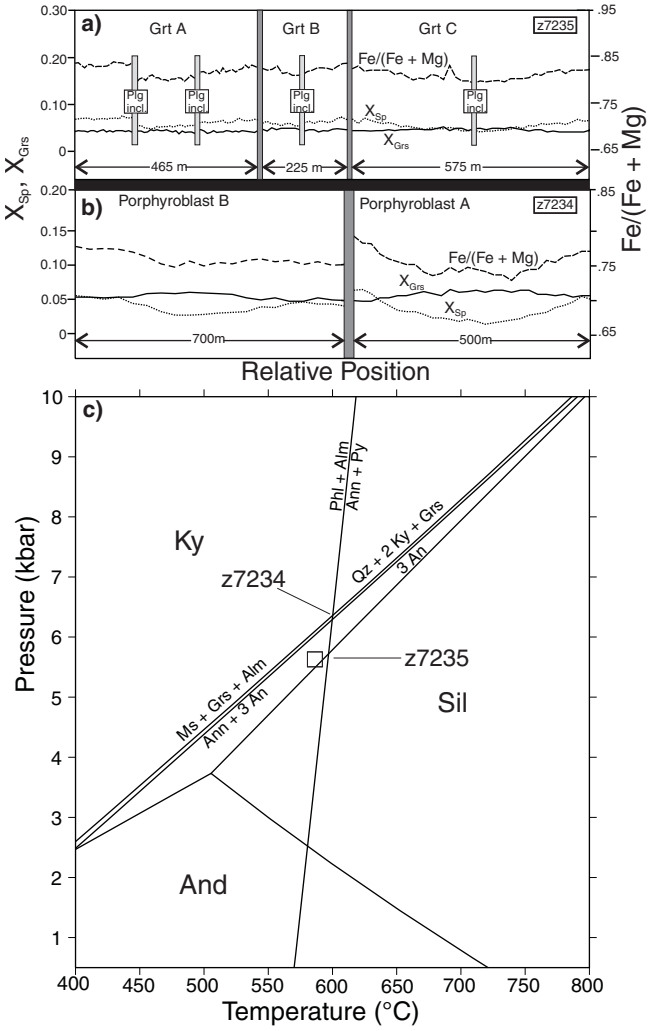

Geochronology

Ion microprobe analyses were obtained from monazite grains in nine thin-section cores (3 mm diameter) mounted in epoxy with a pre-polished mount containing several grains of monazite standard (technique described by Rayner and Stern [2002] and ion microprobe mount illustrated in Fig. 1 of that paper). Fifteen analyses were obtained of 11 different monazite grains that covered a range of textural occurrences within samples z7235 and z7234 (ion microprobe mount no. 238). A 12 by 14 µm diameter primary spot was used for all analyses except two analyses of a small monazite inclusion in a garnet porphyroblast, for which a 7 by 9 µm spot was used. Most monazite grains appear featureless with backscatter electron (BSE) or cathodoluminesence imaging. Analytical techniques were described by Stern and Sanborn (1998) and Stern and Berman (2000), except that energy filtering was used to eliminate ^{204}Pb isobars.

The U-Pb isotopic data for monazite grains are presented in Table 2 and illustrated in Figure 5. The dated monazite grains in sample z7234 are inclusions within foliation-parallel biotite (z7234a-M4 and -M5, Fig. 6a), staurolite

Figure 4. *Electron microprobe and thermobarometric data for samples z7234 and z7235:* ***a)*** *chemical profiles across garnet porphyroblasts in sample z7235;* ***b)*** *chemical profiles across garnet porphyroblasts in sample z7234;* ***c)*** *calculated P-T results. Alm, almandine; An, anorthite; And, andalusite; Ann, annite; Grs, grossular; Grt, garnet; Ky, kyanite; Ms, muscovite; Phl, phlogopite; Py, pyrope; Qz, quartz; Sil, sillimanite.*

Table 2. Sensitive high-resolution ion microprobe U-Pb isotopic data for monazite grains, samples z7234, z7235, z6856, and z6857.

Spot name	Loc[(a)]	U (ppm)	Th (ppm)	Th/U	Pb (ppm)	^{204}Pb (ppb)	^{204}Pb/^{206}Pb	±^{204}Pb/^{206}Pb	f^{206}	^{208}Pb/^{206}Pb
Lab no. z7234				Field no. 86-TXD-047			UTM = 602801, 6989736 Grid Zone 15			
a-M2.1	Ky	7771	42005	5.40558	6161	29	1.29E-05	1.04E-05	2.00E-04	1.6427
a-M4.1	Bt	7769	33991	4.37537	5322	27	1.24E-05	8.05E-06	1.90E-04	1.3196
a-M4.2	Bt	6999	32161	4.59506	4918	37	1.91E-05	7.63E-06	2.90E-04	1.3947
a-M4.3	Bt	14013	56894	4.05992	9331	15	3.72E-06	1.08E-05	6.00E-05	1.2415
a-M5.1	Bt	12791	61352	4.79645	9309	44	1.24E-05	4.68E-06	1.90E-04	1.4824
a-M5.2	Bt	9049	41679	4.60590	6457	10	3.72E-06	1.08E-05	6.00E-05	1.3915
b-M5.1	St	11535	43465	3.76808	7463	62	1.90E-05	5.71E-06	2.90E-04	1.1683
c-M5.1	Ky	8118	36444	4.48907	5768	47	2.04E-05	1.21E-05	3.10E-04	1.3604
Lab no. z7235				Field no. 86-TX-082			UTM = 588822, 6998515 Grid Zone 15			
a-M1.1	Ky	10809	51434	4.75850	7849	56	1.85E-05	6.68E-06	2.80E-04	1.4343
a-M2.1	Gt	10446	49964	4.78332	7712	324	1.08E-04	6.83E-05	1.65E-03	1.4337
a-M2.2	Gt	7857	22115	2.81467	4206	445	2.05E-04	9.04E-05	3.14E-03	0.8124
b-M3.1	Bt	8900	49416	5.55232	7119	119	4.74E-05	1.02E-05	7.30E-04	1.6907
b-M2.1	Bt	9145	47280	5.17031	7033	59	2.27E-05	7.24E-06	3.50E-04	1.5637
c-M2.1	Ky	7504	34638	4.61583	5328	12	5.67E-06	1.24E-05	9.00E-05	1.3866
c-M1.1	Bt	9980	50226	5.03255	7506	30	1.07E-05	5.27E-06	1.60E-04	1.5066
Lab no. z6856				Field no. 89-TXJ-290			UTM = 424154, 6948747 Grid Zone 15			
a-Mz6.1	St	7651	133962	17.5101	14010	213	9.65E-05	1.95E-05	1.81E-03	5.1784
a-Mz7a.1	St	8153	136430	16.7336	14154	155	6.84E-05	1.56E-05	1.29E-03	5.0882
a-Mz7b.1	St	6227	116617	18.7266	12304	179	1.02E-04	3.34E-05	1.92E-03	5.8235
a-Mz8.1	I	4644	47389	10.2038	6587	159	9.48E-05	2.28E-04	1.78E-03	2.7997
Lab no. z6857				Field no. 97-BLB-030			UTM = 423300, 6948300 Grid Zone 15			
Mz3b.1	I	12137	68864	5.67396	9560	275	7.98E-05	2.45E-05	1.50E-03	1.6410
Mz4.1	I	15092	48520	3.21492	8674	54	1.31E-05	1.13E-05	2.50E-04	0.9708
Mz11.1	I	4637	43453	9.37037	4538	123	1.03E-04	4.71E-05	1.93E-03	2.6536
Mz11.2	I	6454	8009	1.24087	2399	72	4.49E-05	2.91E-05	8.40E-04	0.3780
Mz3a.1	Bt	8534	40096	4.69813	5798	22	1.00E-05	1.00E-05	1.90E-04	1.4457

Uncertainties reported at one sigma and are calculated by numerical propagation of all known sources of error (Stern and Berman, 2000).
(a) textural location: I = interstitial; others are inclusions in kyanite (Ky), biotite (Bt), staurolite (St), and garnet (Grt)
(b) mole fraction of total ^{206}Pb that is due to common Pb; data have been corrected for common Pb according to procedures outlined in Stern and Sanborne (1998).
(c) concordance = 100 x (^{206}Pb/^{238}U age)/(^{207}Pb/^{206}Pb age)

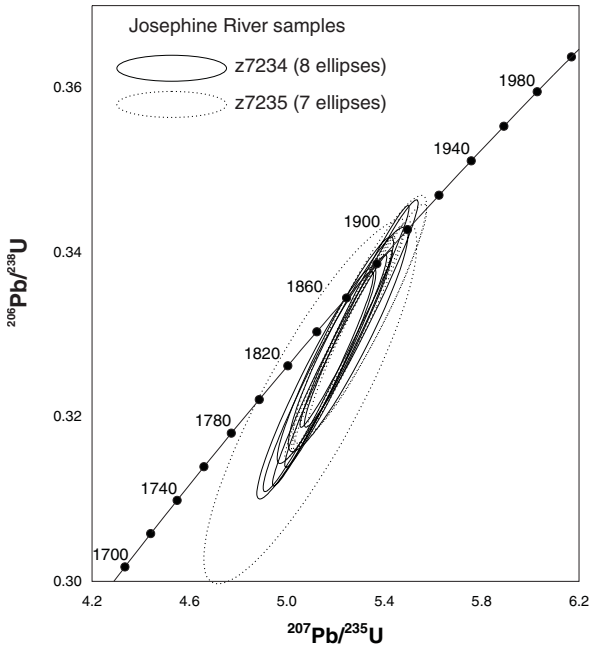

Figure 5.

Concordia diagram for metamorphic monazite analyzed by SHRIMP in situ in samples z7235 and z7234 of the Josephine River belt.

Table 2. (cont.)

Spot name	Loc[(a)]	±^{208}Pb/^{206}Pb	^{206}Pb/^{238}U	±^{206}Pb/^{238}U	^{207}Pb/^{235}U	±^{207}Pb/^{235}U	^{207}Pb/^{206}Pb	±^{207}Pb/^{206}Pb	Apparent ages (Ma) ^{206}Pb/^{238}U	±^{206}Pb/^{238}U	^{207}Pb/^{206}Pb	±^{207}Pb/^{206}Pb	Conc[(c)] (%)
Lab no. z7234					Field no. 86-TXD-047				UTM = 602801, 6989736 Grid Zone 15				
a-M2.1	Ky	0.0156	0.333	0.006	5.31	0.10	0.1157	0.0005	1851	27	1891	8	98
a-M4.1	Bt	0.0098	0.326	0.006	5.18	0.10	0.1153	0.0005	1817	28	1884	7	96
a-M4.2	Bt	0.0151	0.324	0.006	5.12	0.10	0.1146	0.0007	1810	28	1874	11	97
a-M4.3	Bt	0.0131	0.327	0.005	5.21	0.09	0.1156	0.0004	1824	26	1889	7	97
a-M5.1	Bt	0.0101	0.324	0.005	5.13	0.09	0.1147	0.0005	1811	27	1875	9	97
a-M5.2	Bt	0.0219	0.329	0.006	5.25	0.10	0.1156	0.0008	1836	27	1890	13	97
b-M5.1	St	0.0085	0.328	0.006	5.20	0.10	0.1149	0.0007	1829	27	1879	10	97
c-M5.1	Ky	0.0147	0.332	0.006	5.28	0.09	0.1152	0.0004	1849	27	1884	6	98
Lab no. z7235					Field no. 86-TX-082				UTM = 588822, 6998515 Grid Zone 15				
a-M1.1	Ky	0.0081	0.330	0.006	5.25	0.10	0.1156	0.0005	1836	27	1889	8	97
a-M2.1	Gt	0.0322	0.335	0.009	5.44	0.18	0.1177	0.0020	1862	41	1922	31	97
a-M2.2	Gt	0.0307	0.322	0.009	5.10	0.18	0.1148	0.0020	1799	44	1877	32	96
b-M3.1	Bt	0.0097	0.330	0.006	5.26	0.09	0.1156	0.0004	1837	27	1889	6	97
b-M2.1	Bt	0.0105	0.332	0.006	5.33	0.10	0.1164	0.0007	1848	27	1902	11	97
c-M2.1	Ky	0.0099	0.328	0.006	5.22	0.09	0.1152	0.0004	1831	27	1883	7	97
c-M1.1	Bt	0.0179	0.332	0.006	5.30	0.11	0.1158	0.0009	1847	30	1893	15	98
Lab no. z6856					Field no. 89-TXJ-290				UTM = 424154, 6948747 Grid Zone 15				
a-Mz6.1	St	0.0306	0.336	0.004	5.26	0.09	0.1135	0.0012	1867	21	1857	19	101
a-Mz7a.1	St	0.0365	0.323	0.004	5.02	0.08	0.1126	0.0010	1806	19	1842	16	98
a-Mz7b.1	St	0.0518	0.329	0.005	5.16	0.10	0.1139	0.0014	1832	22	1863	23	98
a-Mz8.1	I	0.0665	0.419	0.013	6.31	0.34	0.1091	0.0043	2258	60	1785	73	127
Lab no. z6857					Field no. 97-BLB-030				UTM = 423300, 6948300 Grid Zone 15				
Mz3b.1	I	0.0105	0.331	0.004	5.09	0.08	0.1116	0.0008	1844	20	1825	13	101
Mz4.1	I	0.0056	0.320	0.004	4.93	0.06	0.1118	0.0006	1788	18	1829	10	98
Mz11.1	I	0.0404	0.300	0.005	4.66	0.13	0.1125	0.0022	1693	27	1840	36	92
Mz11.2	I	0.0066	0.290	0.005	4.42	0.11	0.1105	0.0016	1640	25	1808	27	91
Mz3a.1	Bt	0.0221	0.307	0.005	4.78	0.10	0.1129	0.0011	1727	24	1846	18	94

Uncertainties reported at one sigma and are calculated by numerical propagation of all known sources of error (Stern and Berman, 2000).
(a) textural location: I = interstitial; others are inclusions in kyanite (Ky), biotite (Bt), staurolite (St), and garnet (Grt)
(b) mole fraction of total ^{206}Pb that is due to common Pb; data have been corrected for common Pb according to procedures outlined in Stern and Sanborne (1998).
(c) concordance = 100 x (^{206}Pb/^{238}U age)/(^{207}Pb/^{206}Pb age)

Analyzed monazite grains in sample z7235 are inclusions within S_2-parallel biotite (z7235c-M1, Fig. 6d), kyanite (z7235a-M1, Fig. 6e), and garnet (z7235a-M2, Fig. 6f). All analyses are nominally 96–98% concordant, but overlap concordia within error. Eight analyses of five monazite grains in sample z7234 yield a weighted mean ^{207}Pb/^{206}Pb age of 1884 ± 6 Ma (2σ; mean square of weighted deviates [MSWD] = 0.54). Seven analyses of six monazite grains in sample z7235 give a weighted mean ^{207}Pb/^{206}Pb age of 1889 ± 7 Ma (2σ; MSWD = 0.61). All monazite analyses from both samples constitute a single statistical age population with a weighted mean ^{207}Pb/^{206}Pb age of 1886 ± 6 Ma (2σ; MSWD = 0.63).

Radiogenic mineral inclusions strictly provide a maximum age for host mineral growth. The presence of planar crystal boundaries without significant embayments on monazite inclusions may be indicative, however, of near-synchronous host-mineral crystallization, such that monazite inclusions are armoured from subsequent resorption reactions (Stern and Berman, 2000). Most monazite analyzed in these two samples displays some planar and some jagged crystal edges. Evidence of mechanical rounding, expected for monazite grains of detrital origin, was not noted, and the grains are all interpreted to be metamorphic. The single monazite age population suggests that these grains crystallized together with host minerals during one progressive metamorphic event that culminated with S_2 fabric development. The present dataset provides, however, only a minimum age for S_1 and garnet porphyroblasts that may have grown during S_1 fabric development. Two analyses of a near-euhedral monazite inclusion within a garnet porphyroblast that contains randomly oriented inclusions (z7235a-M2; Fig. 6f) yield ^{207}Pb/^{206}Pb ages that are not statistically different from the other monazite ages, suggesting that the growth of this garnet was likely not significantly earlier than other minerals. In summary, the 1886 ± 6 Ma age is interpreted to represent the best age estimate for the Barrovian mineral assemblage and S_2 fabric in the samples from the Josephine River belt.

HAPPY LAKE SUPRACRUSTAL BELT

Geology

The Happy lake (unofficial name, not to be confused with Happotiyik Lake) area (Irwin, 1997), located some 40 km north-northeast of Kaminak Lake (Fig. 2), is underlain by a southwest-trending belt of amphibolite-facies schist and tectonite interpreted to be derived from a dominantly sedimentary protolith. These rocks are distinct in the Kaminak Lake region, not only for their higher strain and metamorphic grade relative to those to the south (e.g. Quartzite Lake) and west (e.g. Victory Lake), but also for their compositional diversity. They are dominated by metapsammite and semipelite, with lesser impure quartzite and pelite, minor orthoquartzite beds, and rare 3 cm thick carbonate layers associated with some quartzite.

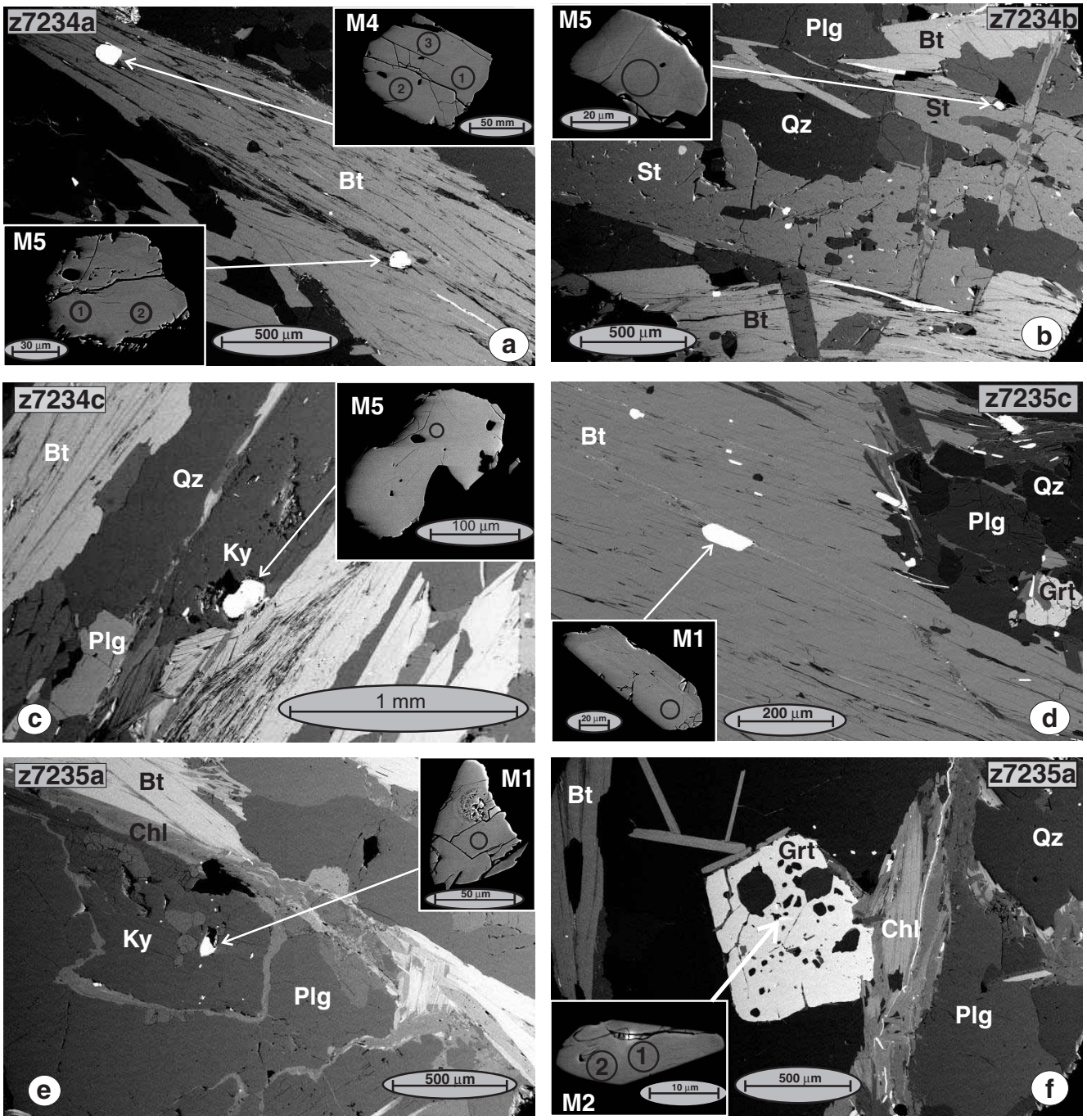

Figure 6. *Textural location of analyzed monazite grains, within* ***a)*** *within S_2-aligned biotite,* ***b)*** *staurolite, and* ***c)*** *kyanite of sample z7234; and within* ***d)*** *biotite (S_2-aligned),* ***e)*** *kyanite, and* ***f)*** *garnet of sample z7235. Abbreviations: Bt, biotite; Chl, chlorite; Grt, garnet; Ky, kyanite; Plg, plagioclase; Qz, quartz; St, staurolite.*

The Happy lake metasedimentary rocks are structurally transposed, exhibiting one main strong schistosity (S_1), parallel to compositional layering (S_0; Hanmer et al., 1998). The S_1 foliation and bedding are isoclinally to openly folded about steep to shallowly plunging, west-southwest-trending F_2 folds (fold axes oriented 230–245°/25–45°; Fig. 7a). The S_1 foliation is strongly reactivated and accentuated on F_2 fold limbs, effectively making it locally an S_2 foliation. An axial-planar S_2 is not pervasively developed in the axial-planar regions of F_2 fold closures, except in micaceous horizons, but S_2 crenulations are common in quartz-rich layers. The S_1 foliation on the limb of a large F_2 fold trends 240° and dips 85°N. A more sparsely developed crenulation cleavage (S_3), trending 040°, overprints the F_2 folds (Fig. 7b).

About 2 km south of Happy lake, the schist changes from pelite-, psammite-, and quartzite-dominated to heterogeneously layered, potentially highly strained, garnet amphibolite that contains granitoid sheets and very rare quartz-rich layers. Shallowly plunging F_2 folds have similar orientation to those in the metasedimentary rocks, suggesting that S_1 is equivalent in the amphibolitic and metasedimentary rocks. Decussate hornblende needles overgrow the F_2 folds. When the effects of F_2 folding are accounted for, the intense S_1 foliation observed in the amphibolite has a shallowly south-dipping attitude. This potential high-strain foliation may be associated with a shear zone that juxtaposed the Happy lake metasedimentary rocks with a crustal block, exposed 4 km to the south, that consists of ca. 2.71–2.68 Ga Kaminak Group and unconformably overlying Paleoproterozoic (ca. 2.45–2.1 Ga) lower Hurwitz Group rocks, both at greenschist-facies metamorphic grade.

Similar geological relationships approximately 70 km west of Happy lake (Aspler et al., 2000) suggest that this shear zone may extend to the MacKenzie Lake area (Mc in Fig. 2). In this region, greenschist-facies, kyanite-bearing Proterozoic quartzite of the lower Hurwitz Group (formerly known as the 'MacKenzie Lake metasediments') and its Archean Kaminak Group basement are bounded to the north (structurally downward) by a subhorizontal to very shallowly south-dipping, high-strain foliation carrying an intense north-trending extension lineation (Aspler et al., 2000). A minimum age for this high-strain fabric is given by a crosscutting, weakly foliated, ca. 1.83 Ga granite (Davis, unpublished data, 2002). The high-strain zone is likely younger than ca. 2.45 Ga because it forms the southern boundary of a gneiss and migmatite domain in which ca. 2.45 Ga Kaminak dykes (Heaman, 1994) are highly deformed and metamorphosed (Davidson, 1970).

Metamorphism

The lowest variance assemblage in metapelitic rocks consists of garnet-kyanite-staurolite-muscovite-biotite-plagioclase-quartz-ilmenite-pyrite. Within the F_2 fold closures, garnet porphyroblasts overgrow straight S_1 inclusion trails. These garnets are oppositely rotated on the limbs of the F_2 folds, illustrating that S_1 predates this generation of garnet, whereas

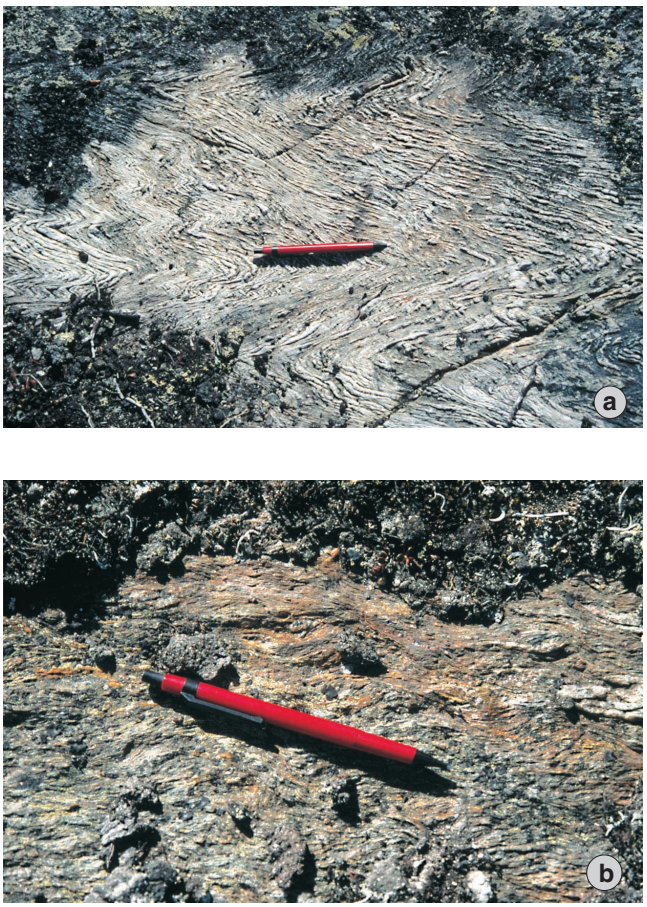

Figure 7. *Metasedimentary rocks near Happy lake:* ***a)*** *F_2 folds of S_1 differentiated layering in Happy lake quartz-rich psammite, with well-developed S_2 crenulations;* ***b)*** *S_3 crenulations overprinting S_1-S_2 schistosity and kyanite in semipelitic horizon.*

F_2 folds postdate it. Similarly, S_2 fabrics are commonly observed enveloping M_2 porphyroblasts of garnet and staurolite, within which S_1 inclusion trails are at a high angle to the enveloping S_2. It is possible that the staurolite crystallization slightly postdated garnet growth, because S_1 inclusion trails are slightly curved in staurolite (Fig. 8a), as opposed to straight in garnet. Kyanite porphyroblasts of M_2 are also aligned with, and enveloped by, the S_2 fabric. The occurrence of S_1 kyanite that has been bent into a fold with its axial plane parallel to S_2 (Fig. 8b; Brown, 1998) suggests that S_1 and S_2 may have developed during a single Barrovian metamorphic event.

Outcrop and petrographic observations demonstrate multiple generations of staurolite relative to S_2 fabric development (Brown, 1998). The first recognizable generation (M_2) overgrew S_1 and was wrapped by S_2. The second generation (M_3) crosscuts the S_2 fabric and is aligned in the S_3 orientation. Lobate embayments on garnet rims are interpreted to be the result of resorption via the reaction (Brown, 1998):

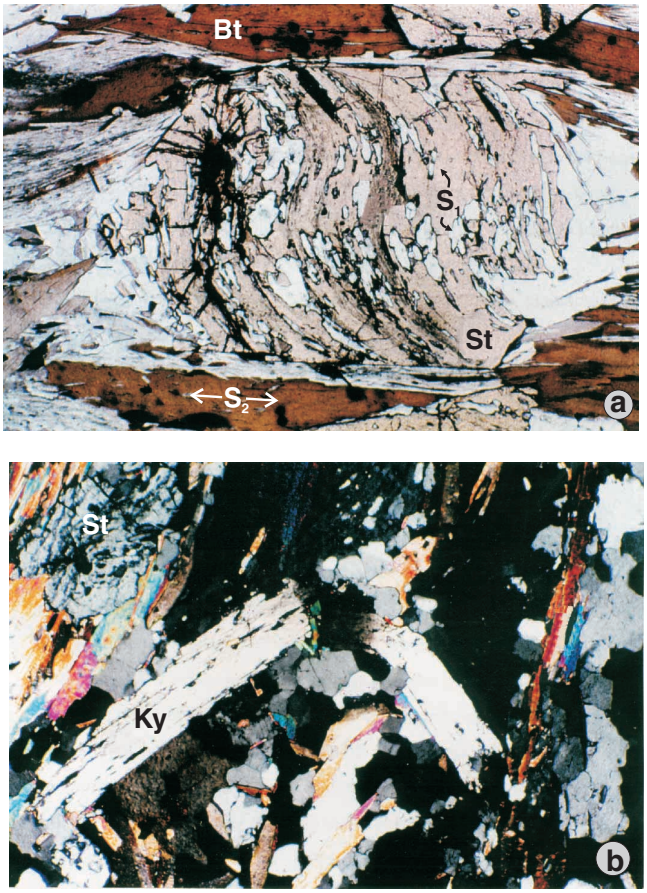

Figure 8. *Happy lake metapelite containing* ***a)*** *S_2-aligned staurolite porphyroblast with curved S_1 inclusion trails, and* ***b)*** *S_1 kyanite folded by S_2 (*adapted from *Brown, 1998). Bt, biotite; Ky, kyanite; St, staurolite.*

$$\text{garnet} + \text{kyanite} + \text{biotite} + \text{quartz} \rightarrow \text{staurolite } (M_3) + \text{muscovite} + \text{plagioclase} \quad (1)$$

Quantitative chemical analyses and P-T estimates were obtained by Brown (1998) for a metapelitic schist and are summarized here. Garnet porphyroblasts, approximately 0.8 mm in diameter, display typical, bell-shaped, prograde growth-zoning profiles, with core-to-rim decreases in CaO (X_{Ca} = 0.20–0.05), MnO (X_{Mn} = 0.10–0.01), and Fe/(Fe+Mg). Forward modelling calculations demonstrate that these composition trends are consistent with prograde garnet growth with increasing or slightly decreasing pressure (Spear, 1993). Thermobarometric calculations yield peak conditions of 585°C and 5.6 kbar, and suggest a clockwise P-T path that may have passed through approximately 565°C and 8.4 kbar (Brown, 1998). Given the incompatibility of simultaneous garnet and plagioclase growth on most P-T paths (e.g. Spear, 1993), the more calcic rims (approx. 10 mole % An) generally observed for matrix plagioclase were likely produced during a later metamorphic event (M_3) that produced partial garnet resorption. Pressure-temperature estimates for M_3 garnet resorption, 4.5 kbar and 575°C, plot in the sillimanite stability field. The lack of observed sillimanite in the Happy lake rocks is consistent with garnet+kyanite resorption via reaction (1).

Two rocks collected from nearby outcrops (<1 km) provided the targets for geochronological analysis. A hand sample of semipelitic schist (sample z6856; field no. 99-TXJ-290a) lacks kyanite but is otherwise as described above. Large blades of kyanite were observed within 1 m of this specimen location. In metapsammite (sample z6857; field no. 97BLB-030), scattered garnet porphyroblasts contain straight inclusion trails that are parallel to the biotite-defined S_2 foliation that envelops them.

Geochronology

Ion microprobe analyses were obtained from two polished rock chips mounted together with several grains of monazite standard (ion microprobe mount #156). A 7 by 9 µm diameter primary spot was used to obtain nine analyses from monazite grains that showed different textural relationships in the two rocks. Monazite is very sparse and small (<15 µm) in sample z6856 and, although no grains were found within kyanite or garnet, several monazite inclusions in S_2 staurolite were located. More abundant monazite in sample z6857 forms interstitial grains as well as inclusions within foliation-parallel biotite. Most grains in both rocks appear uniform under BSE or cathodoluminesence imaging.

The U-Pb isotopic data for monazite grains are presented in Table 2 and illustrated in Figure 9. All analyses for both rocks range from 91–126% concordant, and define a discordia regression line with upper intercept of 1836 ± 14 Ma and lower intercept of 80 Ma (Fig. 9). All analyses can be treated statistically as a single population with a weighted mean $^{207}Pb/^{206}Pb$ age of 1835 ± 11 (2σ) Ma. Given the

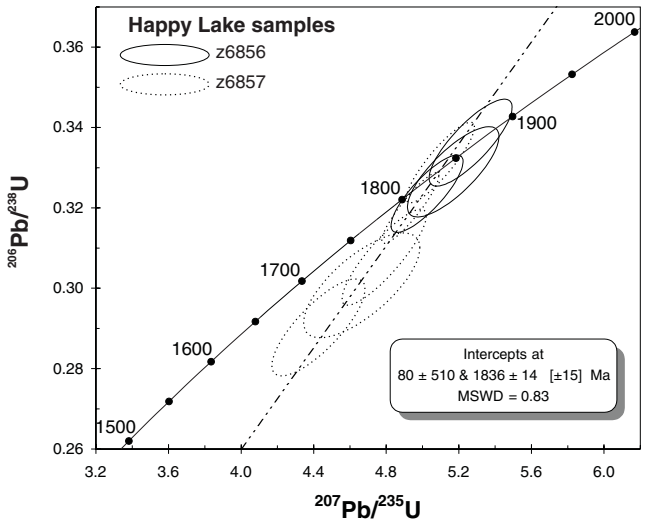

Figure 9. *Concordia diagram for metamorphic monazite analyzed by SHRIMP in situ in Happy lake samples z6856 and z6857.*

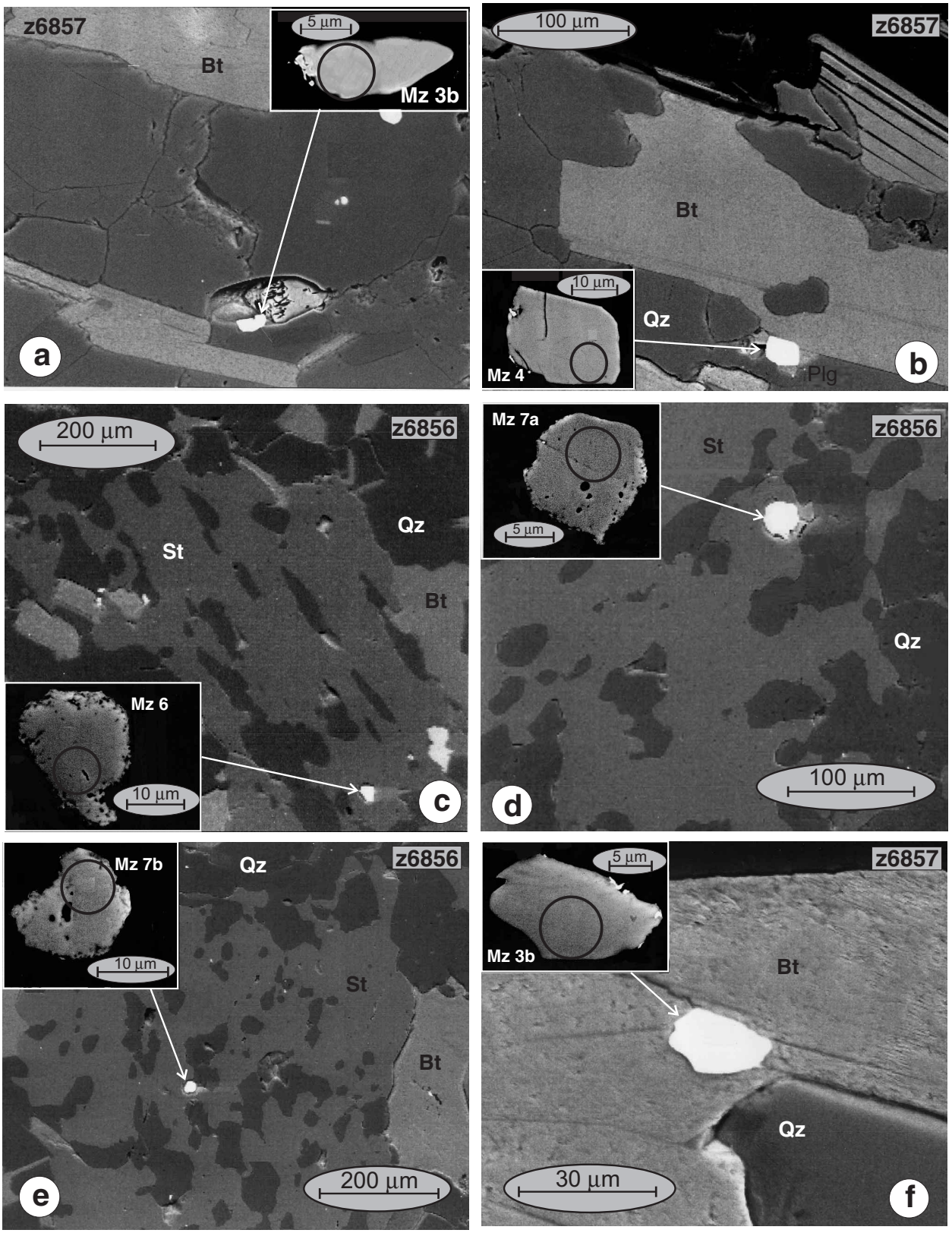

Figure 10. *Textural location of analyzed monazite grains:* ***a)*** *and* ***b)*** *ca. 1.83 Ga grain boundary monazite;* ***c)****,* ***d)****, and* ***e)*** *ca. 1.84–1.86 Ga monazite inclusions in S_2 staurolite containing S_1 fabric;* ***f)*** *ca. 1.84 Ga monazite inclusion in S_2-aligned biotite. Bt, biotite; Mz, monazite; Plg, plagioclase; Qz, quartz; St, staurolite.*

mean $^{207}Pb/^{206}Pb$ age of 1835 ± 11 (2σ) Ma. Given the structural and petrographic evidence discussed above for two metamorphic and three deformation events, however, it is important to note a possible correlation between age and textural setting. The four oldest ages (1842–1863 Ma; average age of 1850 ± 18 Ma) come from the following texturally 'older' grains: three grains that are inclusions within S_2 staurolite porphyroblasts containing an internal fabric (S_1) that is either parallel or at a high angle to the external S_2 foliation (z6856-Mz6, -Mz7a, and -Mz7b, Fig. 10c–e); and a fourth grain (z6857-Mz3b, Fig. 10f) that occurs on a boundary between biotite grains that form the S_2 foliation. The five youngest ages (1785–1840 Ma; weighted average age [excluding spot 8.1] of 1826 ± 15 Ma) were obtained from monazite at grain boundaries of matrix minerals (e.g. z6857-Mz3b and -Mz4, Fig. 10a, b), and may postdate M_2 porphyroblasts. If this correlation is correct, then at least two periods of metamorphic monazite growth are suggested. Ambiguity remains in the interpretation of whether the age of the texturally older monazite is associated with the S_1 or S_2 fabric. The preferred interpretation is that it would give the age of S_2 (and M_2), based on the assumption that growth of monazite grain z6857-Mz3b was synchronous with that of S_2 biotite, as well as the observation that none of the three monazite inclusions in S_2 staurolite are elongate parallel to the other S_1 inclusions. The younger monazite at grain boundaries would then be associated with the M_3 event. Further support for two distinct populations of monazite ages derives from regional geological arguments discussed below.

DISCUSSION

Recent work in the northwestern Hearne domain (Fig. 1, 2) has outlined a ca. 1.9 Ga, high-pressure (10–14 kbar) region extending from Angikuni Lake (Berman et al., 2002) through Parker and MacQuoid Lakes (Stern and Berman, 2000) into granulite-facies rocks within the Cross Bay complex (Ryan et al., 2000), the Kramanituar complex (Sanborn-Barrie et al., 2001), and the Uvauk complex (Tella et al., 1994; Mills, 2001). Within this high-pressure domain, supracrustal rocks, which previously experienced a tectonometamorphic event at 2.56–2.50 Ga (Berman et al., 2000; Stern and Berman, 2000), underwent static metamorphism at 1.9 Ga. An outstanding question has been whether 1) the crust was thickened only during the ca. 2.5 Ga event and subsequently subjected to a 1.9 Ga thermal overprint (Hanmer and Relf, 2000; Aspler et al., 2001), or 2) ca. 1.9 Ga shortening occurred at higher structural levels than presently exposed in the high-pressure domain (Berman et al., 2000).

Two areas with potential for recording ca. 1.9 Ga mid-crustal shortening are the Josephine River and Happy lake supracrustal belts, both of which contain kyanite-staurolite-garnet assemblages associated with regional fabric development. Geochronological data presented above demonstrate that monazite within the approximately 6 kbar Josephine River samples formed at 1886 ± 6 Ma, likely dating the Barrovian-facies mineral assemblages and the associated S_2 fabric. This date also provides a minimum age for the S_1 fabric and possibly early garnet porphyroblastesis. The association of the S_2 fabric with near-isoclinal F_2 folds observable at thin-section (folded S_1 biotite) and outcrop scale demonstrates that the Barrovian metamorphism developed during an episode of mid-crustal shortening at this time. Thermal and thermomechanical models of Barrovian metamorphism indicate a lag time of 15 to more than 40 m.y. between amphibolite-facies metamorphism and the onset of crustal thickening (e.g. England and Thompson, 1984; Huerta et al., 1996; Jamieson et al., 1998, 2002), thereby implying that compressional shortening in the Josephine River belt initiated prior to ca. 1.9 Ga. The new results for the Josephine River samples therefore establish that ca. 1.9 Ga crustal thickening preceded and accompanied the deep crustal metamorphic culmination within the northwestern Hearne domain, best dated at 1902 ± 2 Ma in deformed, approximately 13 kbar and 850°C gabbroic rocks in the Kramanituar complex (Sanborn-Barrie et al., 2001).

The geochronological results presented in this study indicate that, compared to the Josephine River belt, metamorphic monazite grew significantly later at Happy lake, where all monazite ages can be interpreted as a single 1.84 Ga population. As discussed above, however, the authors favour the interpretation that S_2 and M_2 are dated at 1.85 Ga by the monazite inclusions in S_2 staurolite and biotite, and the S_3-M_3 event is dated at ca. 1.83 Ga by the monazite grains that occur along grain boundaries. The occurrence of S_1 kyanite, in addition to S_2 kyanite, suggests that both phases of deformation may have developed over a relatively short period of time during a single Barrovian metamorphic event. The interpretation of two distinct monazite age populations is supported by comparison of Happy lake metamorphic textures with what is presently known about Paleoproterozoic plutonic activity in the area. The growth of M_3-S_3 staurolite via garnet breakdown reaction (1) at low pressure (*see* 'Metamorphism' section, above) indicates a relatively high-temperature, low-pressure environment that is consistent with emplacement of post-tectonic, ca. 1.83 Ga granitic plutons observed at a similar structural level in the MacKenzie Lake area. This correlation, which requires that D_2 deformation and kyanite-garnet-staurolite growth occurred prior to 1.83 Ga, is also most compatible with a lower temperature, higher pressure environment necessary for Barrovian-style metamorphism.

Field observations described above suggest that a flat-lying, shallowly south-dipping, high-strain zone separates the middle-amphibolite–facies Happy lake rocks from Archean greenschist-facies metavolcanic rocks of the Kaminak belt to the south. This high-strain zone, which appears to be equivalent in age to the S_1 fabric in metasedimentary rocks at Happy lake (ca. ≥1.85 Ga), is interpreted to be the same as that observed near MacKenzie Lake (Fig. 2). The authors suggest that this shear zone, referred to here as the Happy lake shear zone, formed a regionally important boundary separating a northern region, strongly affected by Proterozoic deformation, from a large Archean domain (Kaminak belt) that was protected from significant Proterozoic reworking.

The Happy lake shear zone may extend to the southwest where, prior to later extensional faulting, it could have linked with the Nowyak shear zone (dotted line in Fig. 2) that juxtaposes greenschist-facies Archean metavolcanic rocks of the Yathkyed belt (MacLachlan et al., 2000) with another crustal block that experienced Barrovian-style thickening (approx. 10 kbar and 675°C) prior to ca. 1.82 Ga uplift (ter Meer et al., 2000; ter Meer, 2001). To the east, the Happy lake shear zone could link either with the Pyke fault (dotted line in Fig. 2), which has Paleoproterozoic mineralization and associated deformation (Miller et al., 1995; Tella, 1994; R. Carpenter, pers. comm., 2002), or with an undated high-strain zone mapped on Pangertot Peninsula south of Rankin Inlet (dashed-dotted line in Fig. 2; Tella et al., 1986). The first alternative is consistent with this shear zone demarcating on a regional scale the northern extent of preserved, bonafide Hurwitz Group, while placing in its hanging wall the north-trending Kaminak dykes (Davidson, 1970) that have been recognized only south of the Pangertot Peninsula high-strain zone. In contrast, the east-trending, ca. 2.19 Ga, MacQuoid–Tulemalu dyke swarm (Tella et al., 1997) appears to occur to the north and west of this shear zone, although it should be noted that undated, east-trending gabbro dykes have been mapped in the North Henik Lake area to the south (Aspler and Chiarenzelli, 1997).

The possibility cannot be ruled out that the metamorphic contrast between the central and northwestern Hearne domains may have resulted, in part, from subsequent extensional faulting. The geological contrast between these domains that host different Paleoproterozoic dyke swarms suggests, however, that the Happy lake shear zone may have carried the central Hearne domain northward onto rocks of the northwestern Hearne domain during a Paleoproterozoic thrusting event. If S_1 and S_2 at Happy lake occurred during a single ca. 1.85 Ga metamorphic event, the north-south polarity of shortening, as defined by measured extension lineations at MacKenzie Lake, appears to be most likely related to hinterland deformation driven by the northward subduction that produced the ca. 1.865–1.85 Ga Wathaman continental arc (Meyer et al., 1992). If S_1 is significantly older than S_2, the Happy lake shear zone may be similar in age to the ca. 1.89 Ga deformation and Barrovian metamorphism recorded in the Josephine River belt.

ACKNOWLEDGMENTS

We are very grateful to Maggie Currie for her patient drafting and sharp-eyed monazite hunting; Pat Hunt for assistance with the SEM; Deborah Lemkow for troubleshooting graphics problems; and Katherine Venance for providing excellent microprobe analyses. The help of Richard Stern and Nathalie Morisette was instrumental in acquiring the SHRIMP data. Many thanks as well are due to Nicole Raynor for passing on her hard-won artistry in coring thin sections. We appreciate very helpful reviews provided by Simon Hanmer, Sally Pehrsson, and Richard Stern. The work described in this report was carried out as part of geochronology project P80.

REFERENCES

Ansdell, K.M., Lucas, S.B., Connors, K., and Stern, R.A
1995: Kisseynew metasedimentary gneiss belt, Trans-Hudson Orogen (Canada): back-arc origin and collisional inversion; Geology, v. 23, p. 1039–1043.

Aspler, L.B. and Chiarenzelli, J.R.
1997: Archean and Proterozoic geology of the North Henik Lake area, District of Keewatin, Northwest Territories; *in* Current Research 1997-C; Geological Survey of Canada, p. 145–156.

Aspler, L.B., Armitage, A.E., Ryan, J.J., Hauseux, M., Surmacz, S., and Harvey, B.A.
2000: Precambrian geology, Victory and Mackenzie lakes, Nunavut Territory, and significance of 'Mackenzie Lake metasediments', Paleoproterozoic Hurwitz Group; Geological Survey of Canada, Current Research 2000-C10, 10 p.

Aspler, L.B., Chiarenzelli, J.R., Cousens, B.L., McNicoll, V.J., and Davis, W.J.
2001: Paleoproterozoic intracratonic basin processes, from breakup of Kenorland to assembly of Laurentia: Hurwitz Basin, Nunavut, Canada; Sedimentary Geology, v. 141/142, p. 287–318.

Berman, R.G.
1991: Thermbarometry using multiequilibrium calculations: a new technique with petrological applications; Canadian Mineralogist, v. 29, p. 833–856.
1992: Thermobarometry with estimation of equilibration state (TWEEQU): an IBM-compatible software package; Geological Survey of Canada, Open File 2534.

Berman, R.G. and Bostock, H.H.
1997: Metamorphism in the Northern Taltson magmatic zone, Northwest Territories; Canadian Mineralogist, v. 35, p. 1069–1092.

Berman, R.G., Davis, W.J., Aspler, L.B., and Chiarenzelli, J.R.
2002: Sensitive high-resolution ion microprobe (SHRIMP) U-Pb ages of multiple metamorphic events in the Angikuni Lake area, western Churchill Province, Nunavut; Radiogenic Age and Isotopic Studies: Report 15; Geological Survey of Canada, Current Research 2002-F3.

Berman, R.G., Ryan, J.J., Tella, S., Sanborn-Barrie, M., Stern, R.A., Aspler, L., Hanmer, S., and Davis, W.
2000: The case of multiple metamorphic events in the western Churchill Province: evidence from linked thermobarometric and in-situ SHRIMP data, and jury deliberations; *in* GeoCanada 2000; Geological Association of Canada–Mineralogical Association of Canada, Joint Annual Meeting, Calgary, CD-ROM, abstract 836.

Brown, N.
1998: A metamorphic study of metasedimentary rocks from the Kaminak Lake area, western Churchill Province, Northwest Territories; B.Sc. thesis, Carleton University,Ottawa, Ontario, 48 p.

Davidson, A.
1970: Precambrian geology, Kaminak Lake map-area, District of Keewatin (55L); Geological Survey of Canada, Paper 69-51, 27 p.

Davis, W.J., Hanmer, S., Aspler, L., Sandeman, H., Tella, S., Zaleski, E., Relf, C., Ryan, J., Bermman, R., and MacLachlan, K.
2000: Regional differences in the Neoarchean crustal evolution of the western Churchill Province: can we make sense of it? *in* GeoCanada 2000; Geological Association of Canada–Mineralogical Association of Canada, Joint Annual Meeting, Calgary, CD-ROM, abstract 864.

England, P.C. and Thompson, A.B.
1984: Pressure-temperature-time paths of regional metamorphism, I: heat transfer during the evolution of regions of thickened continental crust; Journal of Petrology, v. 25, p. 894–928.

Hanmer, S.
1997: Geology of the Striding-Athabasca mylonite zone, northern Saskatchewan and southeastern District of Mackenzie, N.W.T.; Geological Survey of Canada, Bulletin 501, 92 p.

Hanmer, S. and Relf, C.
2000: Western Churchill NATMAP Project: new results and potential significance; *in* GeoCanada 2000; Geological Association of Canada–Mineralogical Association of Canada, Joint Annual Meeting, Calgary, CD-ROM, abstract 79.

Hanmer, S., Sandeman, H.A., Rainbird, R.H., Peterson, T.D., Ryan, J.J. and Goff, S.P.
1998: Geology, Heninga Lake–Kogtok River area, Kivalliq region, Northwest Territories; Geological Survey of Canada, Open File Map 3648, scale 1:125 000.

Heaman, L.M.
1994: 2.45 Ga global mafic magmatism: Earth's oldest superplume? *in* Abstracts of the Eighth International Conference on Geochronology, Cosmochronology, and Isotope Geology, (ed.) M.A. Lanphere, G.B. Dalrymple, and B.D. Turrin; United States Geological Survey, Circular 1107, p. 132.

Hoffman, P.F.
1990: Subdivision of the Churchill Province and extent of the Trans-Hudson Orogen; *in* The Early Proterozoic Trans-Hudson Orogen of North America, (ed.) J.F. Lewry and M.R. Stauffer; Geological Association of Canada, Special Paper 37, p. 15–39.

Huerta, A.D., Royden, L.H., and Hodges, K.V.
1996: The interdependence of deformation and thermal processes in mountain belts; Science, v. 273, p. 637–639.

Irwin, D.A.
1997: Geology and mineral occurrences of the Happy Lake area, District of Keewatin (parts of 55 L/9 and 10); Northwest Territories Geological Mapping Division, Map 1997-04, scale 1:50 000.

Jamieson, R.A., Beaumont, C., Fullsack, P., and Lee, B.
1998: Barrovian regional metamorphism: where's the heat? *in* What Drives Metamorphism and Metamorphic Reaction? (ed.) P.J. Treloar and P.J. O'Brien; Geological Society, London, Special Publication 138, p. 23–51.

Jamieson, R.A., Beaumont, C., Nguyen, M.N., and Lee, B.
in press: Interaction of metamorphism, deformation and exhumation in large convergent orogens; Journal of Metamorphic Geology.

MacLachlan, K., Relf, C., and Davis, W.J.
2000: U-Pb geochronological constraints on structures controlling distribution of tectonothermal domains, Yathkyed Lake area, western Churchill Province; *in* GeoCanada 2000; Geological Association of Canada–Mineralogical Association of Canada, Joint Annual Meeting, Calgary, CD-ROM, abstract 751.

Meyer, M.T., Bickford, M.E., and Lewry, J.F.
1992: The Wathaman Batholith: an early Proterozoic continental arc in the Trans-Hudson orogenic belt, Canada; Geological Society of America Bulletin, v. 104, p. 1073–1085.

Miller, A.R., Balog, M.J., and Tella, S.
1995: Oxide iron-formation-hosted lode gold, Meliadine Trend, Rankin Inlet Group, Churchill Province, Northwest Territories; *in* Current Research 1995-C; Geological Survey of Canada, p. 163–174.

Mills, A.
2001: Tectonic evolution of the Uvauk complex, Churchill Province, Nunavut Territory, Canada; M.Sc.thesis, Carleton University, Ottawa, Ontario.

Paul, D., Hanmer, S., Tella, S., Peterson, T.D., and LeCheminant, A.N.
in press: Compilation bedrock geology of part of the western Churchill Province, Nunavut; Geological Survey of Canada, Open File 4236, map at 1:1000 000 scale.

Rayner, N.M. and Stern, R.A.
2002: Improved sample-preparation method for sensitive high-resolution ion-microprobe (SHRIMP) analysis of delicate mineral grains exposed in thin sections; Radiogenic Age and Isotopic Studies: Report 15; Geological Survey of Canada, Current Research 2002-F10.

Ross, G.M., Milkereit, B., Eaton, D., White, D., Kanasewich, E.R., and Burianyk, M.J.A.
1995: Paleoproterozoic collisional orogen beneath the western Canada sedimentary basin imaged by LITHOPROBE crustal seismic-reflection data; Geology, v. 23, p. 195–199.

Ryan, J.J., Davis, W., Berman, R., Sandeman, H., Hanmer, S., and Tella, S.
2000: 2.5 Ga granulite-facies activity and post-1.9 low-grade reactivation along the Big lake shear zone, MacQuoid-Gibson lakes area (Nunavut): a fundamental boundary in the western Churchill Province; *in* GeoCanada 2000; Geological Association of Canada–Mineralogical Association of Canada, Joint Annual Meeting, Calgary, CD-ROM, abstract 924.

Sanborn-Barrie, M., Carr, S.D., and Thériault, R.
2001: Geochronological constraints on metamorphism, magmatism, and exhumation of deep-crustal rocks of the Kramanituar Complex, with implications for the Paleoproterozoic evolution of the Archean western Churchill Province, Canada; Contributions to Mineralogy and Petrology, v. 141, p. 592–612.

Spear, F.
1993: Metamorphic Phase Equilibria and Pressure-Temperature-Time Paths; Mineralogical Society of America, 799 p.

Stern, R.A. and Berman, R.G.
2000: Monazite U-Pb and Th-Pb geochronology by ion microprobe, with an application to in situ dating of an Archean metasedimentary rock; Chemical Geology, v. 172, p. 113–130.

Stern, R.A. and Sanborn, N.
1998: Monazite U-Pb and Th-Pb geochronology by high-resolution secondary ion mass spectrometry; *in* Radiogenic Age and Isotopic Studies: Report 11; Geological Survey of Canada, Current Research 1998-F, p. 1–18.

Tella, S.
1993: Geology, Chesterfield Inlet, District of Keewatin, Northwest Territories; Geological Survey of Canada, Open File 2756, map at 1:250 000 scale.
1994: Geology, Rankin Inlet (55 K/16), Falstaff Island (55 J/13), and Quartzite Island (55 J/11), District of Keewatin, Northwest Territories; Geological Survey of Canada, Open File 2968, colour digital map at 1:50 000 scale.
1995: Geology, Scarab and Baird Bay, District of Keewatin, Northwest Territories; Geological Survey of Canada, Open File 3197, map at 1:50 000 scale.

Tella, S. and Annesley, I.R.
1987: Precambrian geology of parts of the Chesterfield Inlet map area, District of Keewatin; *in* Current Research, Part A; Geological Survey of Canada, Paper 87-1A, p. 25–36.

Tella, S., Annesley, I.R., Borradile, G.J., and Henderson, J.R.
1986: Precambrian geology of parts of Tavani, Marble Island, and Chesterfield Inlet map areas, District of Keewatin, N.W.T.; Geological Survey of Canada, Paper 86-13, 20 p.

Tella, S., LeCheminant, A.N., Sanborn-Barrie, M., and Venance, K.E.
1997: Geology and structure of parts of MacQuoid Lake map area, District of Keewatin, Northwest Territories; *in* Current Research 1997-C; Geological Survey of Canada, p. 123–132.

Tella, S., Roddick, J.C., Schau, M., and Mader, U.
1994: Geochronological constraints on the tectono-metamorphic history of the allochthonous Uvauk gabbro-anorthosite-granulite complex, central Churchill Province, District of Keewatin, N.W.T., Canada; Geological Association Canada–Mineralogical Association of Canada, Joint Annual Meeting, Program with Abstracts, v. 19, p. A111.

Tella, S., Schau, M., Armitage, A.E., Seemayer, B.E., and Lemkow, D.
1992: Precambrian geology and economic potential of the Meliadine Lake–Barbour Bay region, District of Keewatin, Northwest Territories; *in* Current Research, Part C; Geological Survey of Canada, Paper 92-1C, p. 1–11.

ter Meer, M.
2001: Tectonometamorphic history of the Nowyak Complex, Nunavut, Canada; M.Sc. thesis, Carleton University, Ottawa, Ontario, 285 p.

ter Meer, M., Berman, R.G., Relf, C., and Davis, W.J.
2000: Tectonometamorphic history of the Nowyak Complex, Nunavut, Canada; *in* GeoCanada 2000; Geological Association of Canada–Mineralogical Association of Canada, Joint Annual Meeting, Calgary, CD-ROM, abstract 949.

Wheeler, J., Hoffman, P., Card, K., Davidson, A., Sanford, B., Okulitch, A., and Roest, W.
1996: Geological map of Canada; Geological Survey of Canada, Map 1860A, scale 1:5 000 000.

Geological Survey of Canada Project 970006